Electronic Supplementary Information

A Near-Infrared Fluorescence Probe for Accurately Diagnosing Cancer by Sequential Detection of Cysteine and H^+

Zun-Pan She,[a] Wen-Xin Wang,[a] Guo-Jiang Mao,[b] Wen-Li Jiang,[a] Zhi-Qing Wang,[a] Yongfei Li,*[,a,c] and Chun-Yan Li*[,a]

[a] Key Laboratory for Green Organic Synthesis and Application of Hunan Province, Key Laboratory of Environmentally Friendly Chemistry and Applications of Ministry of Education, College of Chemistry, Xiangtan University, Xiangtan, 411105, PR China.

[b] Henan Key Laboratory of Organic Functional Molecule and Drug Innovation, Collaborative Innovation Center of Henan Province for Green Manufacturing of Fine Chemicals, Key Laboratory of Green Chemical Media and Reactions, Ministry of Education, School of Chemistry and Chemical Engineering, Henan Normal University, Xinxiang, 453007, PR China.

[c] College of Chemical Engineering, Xiangtan University, Xiangtan, 411105, PR China.

*Corresponding Author. E-mail: lichunyan79@sina.com (Chun-Yan Li); liyongfei@xtu.edu.cn (Yong-Fei Li)

Table of contents

1. Experimental Section.

Reagents and instruments. Sodium dodecyl sulfate (SDS), cyclohexanone, iodoethane, 1,1,2-trimethybenz[e]indole, phosphorus oxychloride, and acryloyl chloride were purchased from Sigma-Aldrich (St. Louis, USA). All the above chemicals were of analytical reagent grade and used as received.

Nuclear magnetic resonance (NMR) spectra were carried out on a Bruker Avance II NMR spectrometer (Germany). Mass spectrometer (MS) was recorded on a Bruker Autoflex MALDI-TOF mass spectrometer (Germany). Element analysis was done on Perkin Elmer 2400 elemental analyzer (USA). The fluorescence spectra were operated on a Perkin Elmer LS-55 fluorescence spectrometer (USA). The absorption spectra were collected on a Perkin Elmer Lambda 25 UV/Vis spectrophotometer (USA). HPLC was performed on an Agilent 1260 LC system (USA). Fluorescence imaging of cells were carried out by a Nikon confocal fluorescence microscope (Japan). Fluorescence imaging of mice was done on an IVIS Lumina XR small animal optical in vivo imaging system (USA).

General procedure for fluorescence measurement. CyAc solution (200 μM) was obtained by dissolving CyAc in DMSO. Cys solution (1 mM) was obtained by dissolving Cys in pure water. SDS solution (400 mM) was obtained by dissolving SDS in pure water. For the test solution of Cys, CyAc solution (100 μL), SDS solution (200 μL) and appropriate volume of Cys solution were added to PBS buffer (0.01 M, pH 7.4) and diluted to 4 mL. Fluorescence spectra were recorded under 550 nm excitation, and the emission was recorded at 570-900 nm. For the test solution of pH, CyAc solution (100 μL), SDS solution (200 μL) and Cys solution (160 μL) were added in PBS buffer with different pH to a final volume of 4 mL. Fluorescence spectra were recorded under 720 nm excitation, and the emission was recorded at 740-900 nm.

The excitation and the emission slit were all set to 5 nm.

Determination of pK_a. The pK_a of the probe is calculated to be 6.30 following equation (1).

$$pK_a = pH - \log[(F_{max} - F)/(F - F_{min})] \quad (1)$$

Here, F_{max}, F_{min} and F represent the fluorescence intensity at pH 5.0, pH 7.4, and the selected pH, respectively.

Cell incubation and fluorescence imaging. HCT116 cells and FHC cells were obtained from the State Key Laboratory of Chemo/Biosensing and Chemometrics of Hunan University (Changsha, China). The cells were cultured in DMEM and 10% FBS and 1% antibiotics at 37 ºC and 5% CO_2.

For imaging experiments of Cys, the HCT116 cells were treated with 10 μM CyAc at 37 ºC for 30 min. Meanwhile, the HCT116 cells were pretreated with NEM (200 μM) at 37 ºC for 30 min, and incubated with 10 μM CyAc at 37 ºC for another 30 min. Subsequently, different concentrations of Cys (0, 10, 20, 30, 40, 50 μM) were added to NEM-pretreated HCT116 cells and then incubated for 30 min. The cells are all in neutral environment (pH 7.4) and were washed with PBS buffer for three times.

For imaging at different pH, the HCT116 cells were treated with 10 μM CyAc at 37 °C for 30 min, and high K^+ buffer at various pH (7.4, 7.0, 6.5, 6.0, 5.5, 5.0). 15 μg/mL of nigericin was added for 30 min to equilibrate the intracellular and extracellular pH. Subsequently, the HCT116 cells were incubated with $NaHCO_3$ (200 μM) for 30 min. The cells were washed with PBS buffer for three times.

For imaging in normal and cancer cells, the FHC cells and HCT116 cells were treated

with CyAc (10 μM) at 37 °C for 30 min and then washed by PBS buffer for three times.

Fluorescence imaging in mice. All animal operations were performed following the regulations issued by the Ethical Committee of Xiangtan University. Six week-old male BALB/C nude mice were used in all the experiments. The tumor mice model was established by subcutaneously injecting with HCT116 cells. The mice were divided into four groups. The first group was normal mice, injected with CyAc (10 μM) subcutaneously. The second group was tumor mice, injected with CyAc (10 μM) subcutaneously. The third group was tumor mice, injected with $NaHCO_3$ (200 μM) for 1 h, and then injected with CyAc (10 μM) subcutaneously. The fourth group was tumor mice, injected with NEM (200 μM) for 1 h, and then injected with CyAc (10 μM) subcutaneously. All of the mice were anesthetized with chloral hydrate (10% in saline) and placed into the imaging chamber to image.

2. Synthesis of probes.

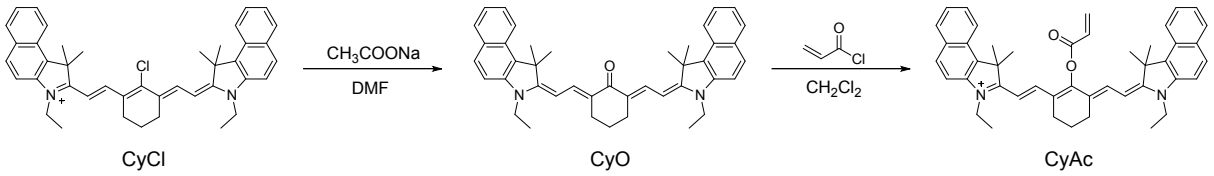

Scheme S1. Synthetic route for CyAc.

Synthesis of CyAc. The synthetic route was depicted in Scheme S1. Compound CyCl was prepared as described previously (Dyes Pigments., 2020, 179, 108402).

Compound CyO. A mixture of CyCl (738 mg, 1 mmol) and sodium acetate (408 mg, 3 mmol) in anhydrous DMF (15 mL) was heated at 90 °C for 6 h under nitrogen atmosphere. The mixture was dissolved in CH_2Cl_2 (50 mL), followed by washing with water for three times and drying by Na_2SO_4. The solvent was removed by evaporation under reduced pressure, and the residue was subjected to silica gel chromatography with CH_2Cl_2/AcOEt (10/1, v/v) as eluent to afford a deep red solid. Yield: 343 mg (58%). ^{1}H NMR (400 MHz, $CDCl_3$): δ 8.35 (d, J = 12.8 Hz, 2H), 8.06 (d, J = 8.8 Hz, 2H), 7.82 (d, J = 8.4 Hz, 2H), 7.78 (d, J = 8.4 Hz, 2H), 7.49 (t, J = 7.6 Hz, 2H), 7.29-7.25 (m, 2H), 7.09 (d, J = 8.4 Hz, 2H), 5.53 (d, J = 13.2 Hz, 2H), 3.86-3.83 (m, 4H), 2.65 (t, J = 5.6 Hz, 4H), 2.02 (s, 12H), 1.92-1.87 (m, 2H), 1.31 (t, J = 6.8 Hz, 6H). ^{13}C NMR (100 MHz, $CDCl_3$): δ 186.1, 163.8, 141.0, 132.8, 129.9, 129.7, 129.4, 129.0, 126.8, 126.2, 122.5, 121.8, 109.1, 91.8, 48.6, 37.1, 29.7, 27.9, 25.9, 22.6, 11.5. MS (TOF): $[M-H]^-$ calcd. 591.3, found 591.5. Elemental analysis (%) calcd. for $C_{42}H_{44}N_2O$: C, 85.09, H, 7.48, N, 4.73; found: C, 85.08, H, 7.50, N, 4.74.

Compound CyAc. To a solution of acryloyl chloride (82 μL, 1 mmol) in anhydrous dichloromethane (10 mL) at 0 °C under nitrogen atmosphere, then CyO (59.2 mg, 0.1 mmol) was added dropwise. The reaction mixture was remained at 0 °C for 1 h, and then stirred at

room temperature for 12 h. The crude product was washed by water three times. The solvent was removed by evaporation under reduced pressure, and the residue was subjected to silica gel chromatography with CH_2Cl_2/CH_3OH (10/1, v/v) as eluent to afford green solid. Yield: 35.6 mg (55%). ^{1}H NMR (400 MHz, DMSO-d_6): δ 8.21 (d, J = 8.0 Hz, 2H), 8.08-8.03 (m, 4H), 7.76-7.70 (m, 4H), 7.63 (d, J = 8.0 Hz, 2H), 7.51-7.47 (m, 2H), 6.89 (d, J = 16.0 Hz, 1H), 6.80-6.73 (m, 1H), 6.53 (d, J = 12.0 Hz, 1H), 6.27 (d, J = 16.0 Hz, 2H), 4.34-4.32 (m, 4H), 2.71 (d, J = 4.0 Hz, 4H), 1.86 (s, 12H), 1.33 (t, J = 16.0 Hz, 8H). ^{13}C NMR (100 MHz, DMSO-d_6): δ 172.9, 172.8, 169.0, 167.4, 164.0, 158.5, 139.8, 138.9, 136.6, 134.0, 131.9, 131.0, 130.4, 129.1, 128.0, 127.1, 125.4, 122.7, 121.4, 112.0, 100.5, 51.0, 37.5, 27.4, 24.2, 19.1, 12.9. MS (TOF): $[M]^+$ calcd. 647.4, found 647.5. Elemental analysis (%) calcd. for $C_{45}H_{47}N_2O_2^+$: C, 83.42, H, 7.31, N, 4.32; found: C, 83.43, H, 7.32, N, 4.31.

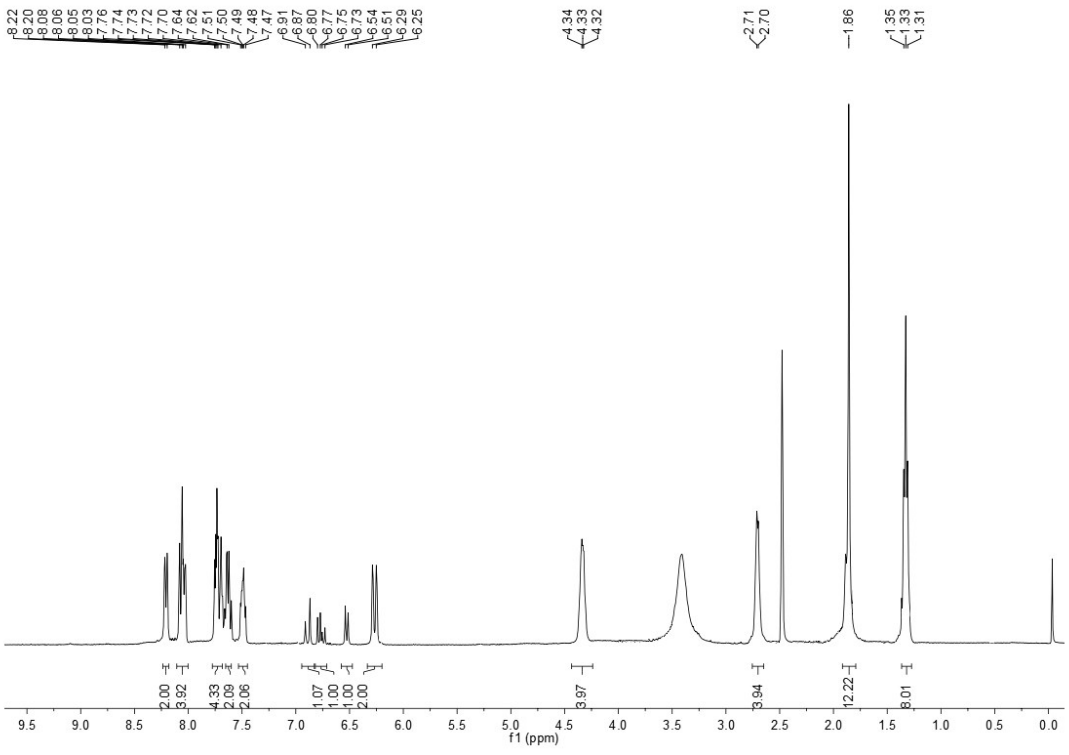

Fig. S1. ^{1}H NMR spectra of CyAc in DMSO-d_6

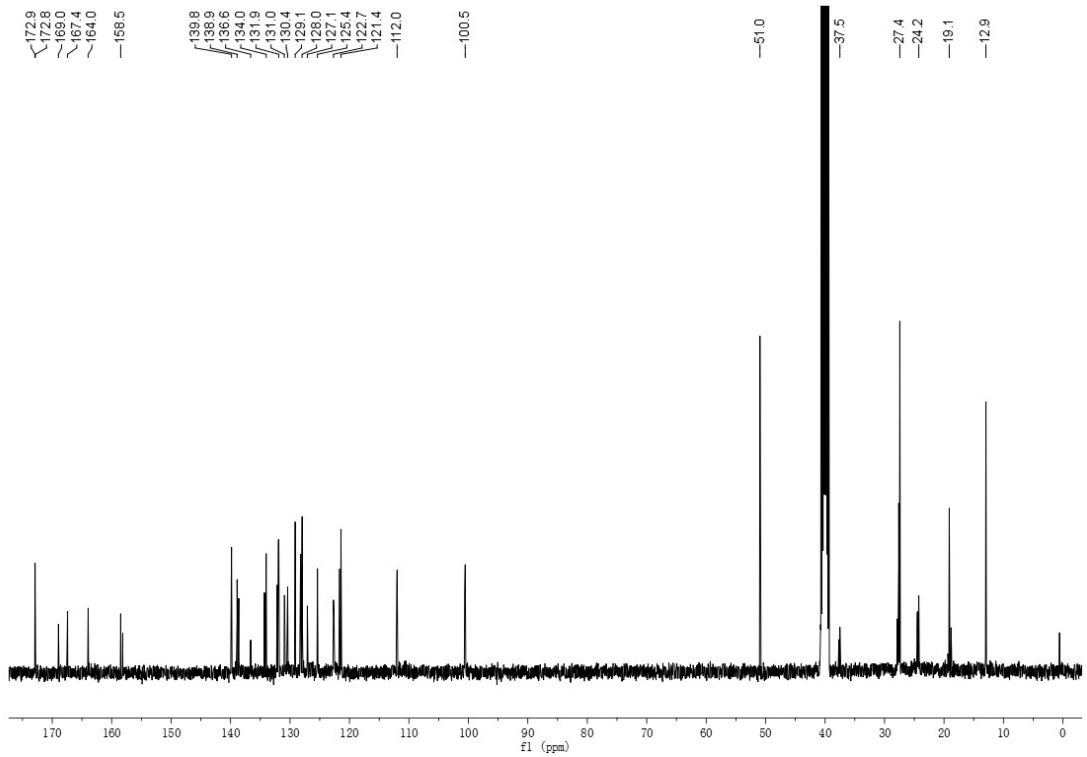

Fig. S2. ^{13}C NMR spectra of CyAc in DMSO-d_6.

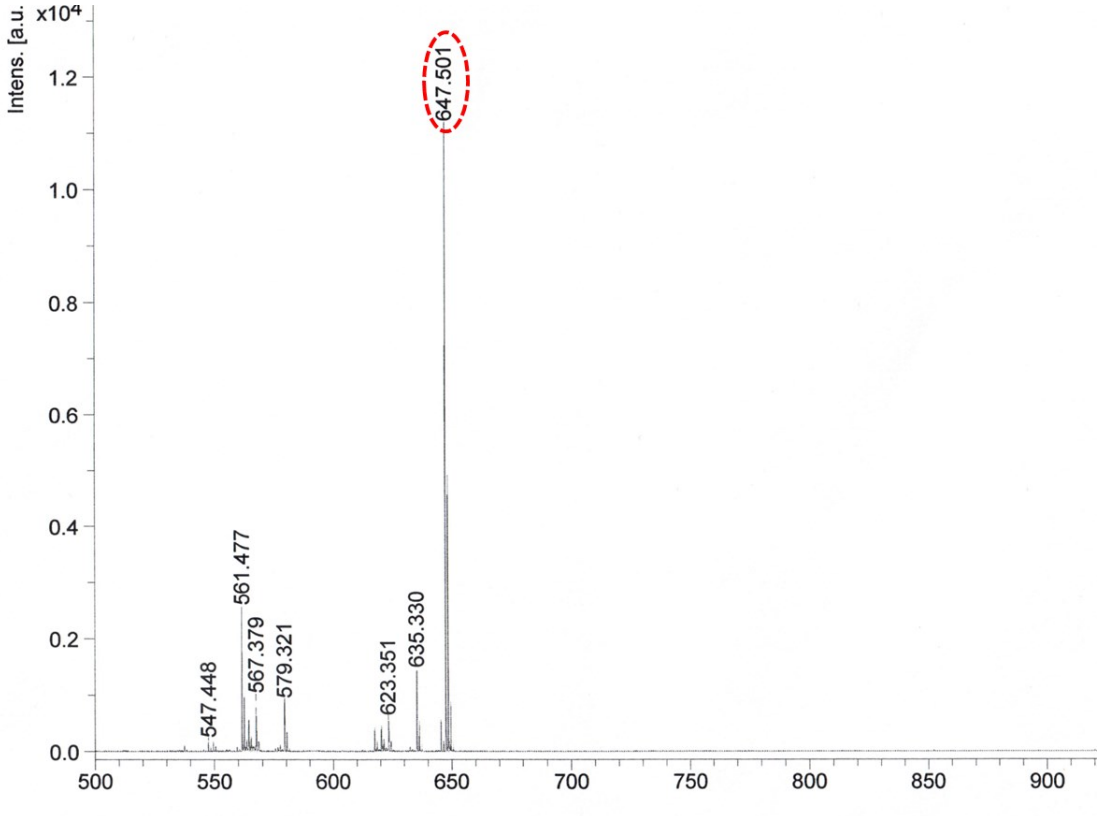

Fig. S3. Mass spectra of CyAc.

3. Spectral data.

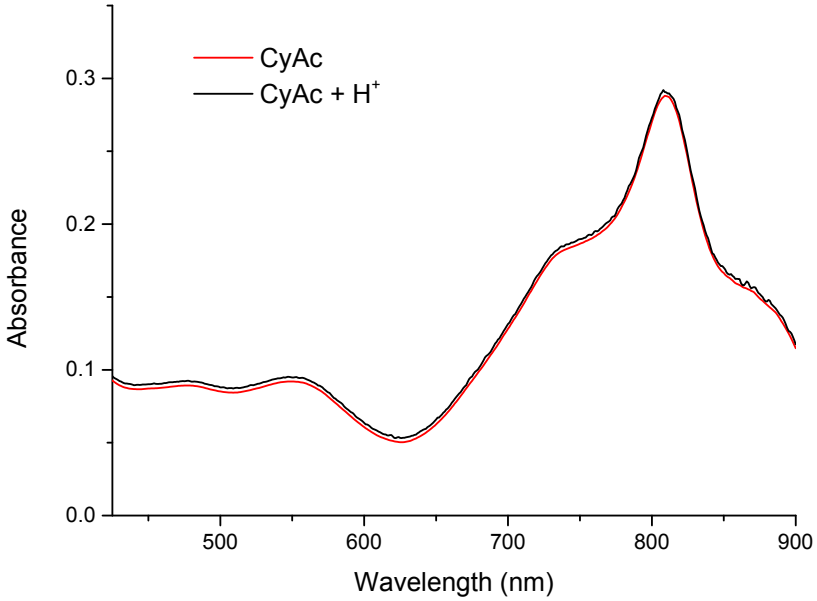

Fig. S4. Absorption spectra of CyAc (5 μM) in PBS buffer (pH 7.4) and PBS buffer (pH 5.0), respectively.

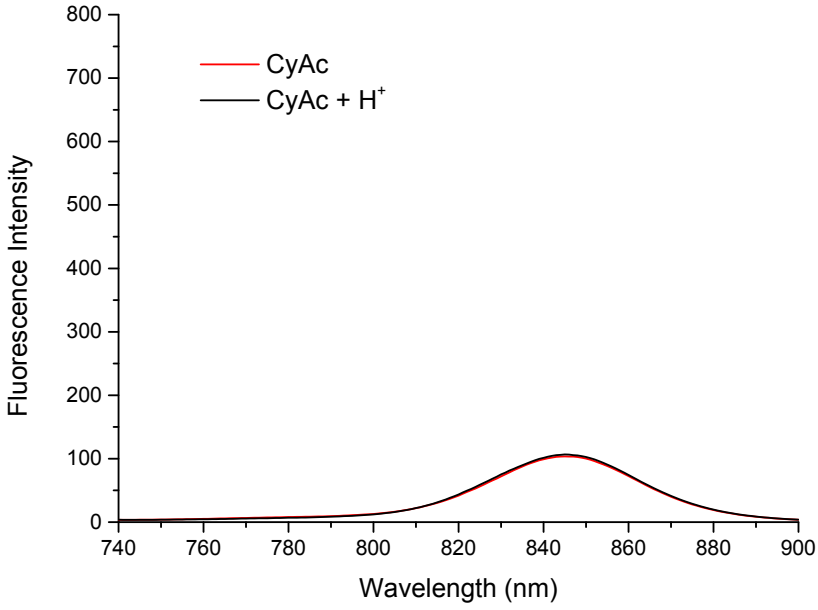

Fig. S5. Fluorescence spectra of CyAc (5 μM) in PBS buffer (pH 7.4) and PBS buffer (pH 5.0), respectively. λ_{ex} = 720 nm.

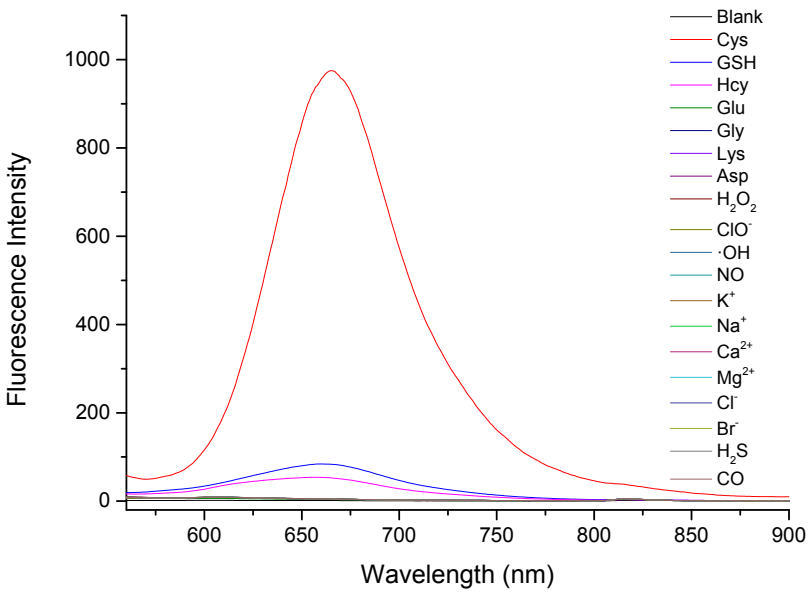

Fig. S6. Fluorescence spectra of CyAc (5 μM) upon the addition of Cys (40 μM) and other analytes (500 μM) in PBS buffer (pH 7.4). λ_{ex} = 550 nm.

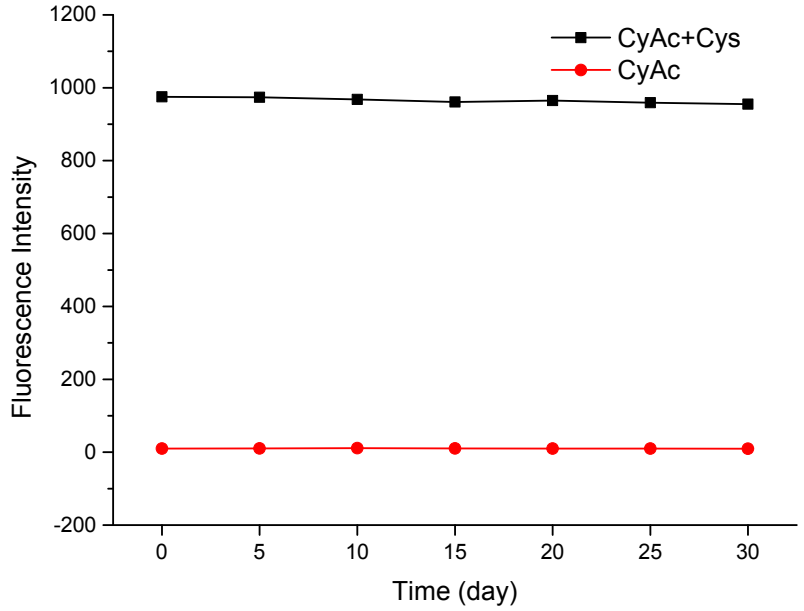

Fig. S7. Fluorescence intensity of CyAc (5 μM) and CyAc upon the addition of Cys (40 μM) in PBS buffer (pH 7.4) in 30 days. λ_{ex} / λ_{em} = 550 / 660 nm.

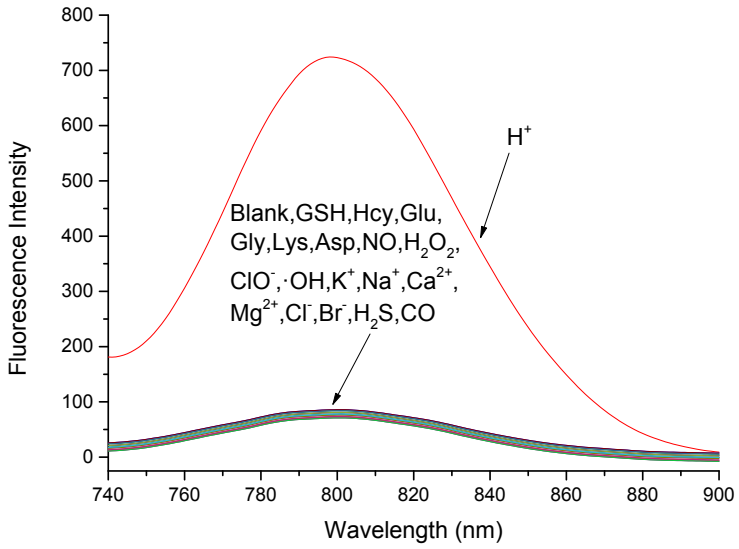

Fig. S8. Fluorescence spectra of CyAc (5 μM) with Cys (40 μM) responding to other analytes (500 μM). λ_{ex} = 720 nm.

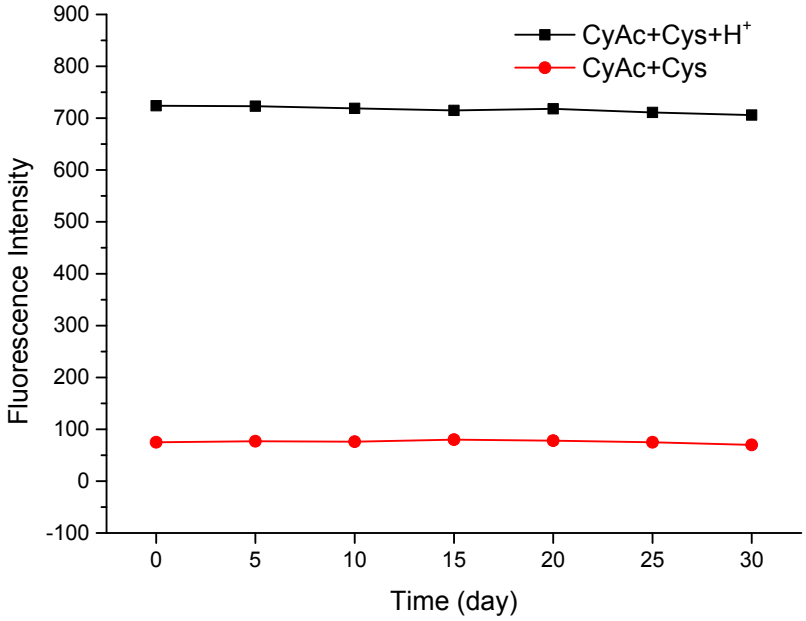

Fig. S9. Fluorescence intensity of CyAc with Cys at pH 5.0 and CyAc with Cys at pH 7.4 in 30 days. λ_{ex} / λ_{em} = 720 / 790 nm.

4. Response mechanism.

According to the above spectral characteristics, a possible response mechanism was given (Scheme S2). CyAc is non-fluorescent at 660nm. In the presence of Cys, the unique adduct and intramolecular cyclization of α,β-unsaturated acrylate leads to the transformation of CyAc into CyO, which shows strong fluorescence. The response mechanism of the probe to Cys was confirmed by HPLC experiments (Fig. S10). CyAc itself displays a signal peak at 2.3 min. After adding Cys, a signal peak at 6.7 min is seen, which shows the same retention time with standard sample of CyO (6.7 min). Moreover, the reaction of CyAc with Cys was analyzed by mass spectra. For CyAc, the peak was at m/z = 647.5 (Fig. S3). Upon adding Cys, the peak at m/z = 647.5 decreases and a new peak at m/z = 591.5 appears (Fig. S11). which is similar to the peak of CyO (m/z = 591.3, Fig. S12). These results well support the proposed response mechanism.

In addition, based on the above spectral evidence, a possible mechanism of CyAc with Cys upon the addition of H^+ was proposed in Scheme S3. Upon the addition of H^+, acidic condition induces the protonation of CyO to get CyOH. CyO itself is non-fluorescent at 790 nm, while CyOH has strong fluorescence, which may be owing to the formation of pull-push π-conjugation system. The specific response mechanism of CyAc with Cys to H^+ was confirmed by mass spectrometry. For CyAc with Cys, the unique peak is at m/z = 591.3, which is corresponding to CyO (Fig. S12). Upon adding H^+, the main peak at m/z = 592.4 corresponding to CyOH appears (Fig. S13), which confirms that the drop of pH leads to the transformation of CyO to CyOH. Subsequently, the density functional theory calculation by the Gaussian 09 package was performed. The optimized structures and the frontier molecular

orbitals for CyO and CyOH were shown in Fig. S14 and Fig. S15. The HOMO-LUMO energy gaps of CyO and CyOH are calculated as 2.25 eV and 2.96 eV, respectively, which therefore serves as the evidence of wavelength changes. These preliminary results indicate that CyAc can specifically and sequentially detect Cys and H^+, which provide a basis for subsequent biological applications.

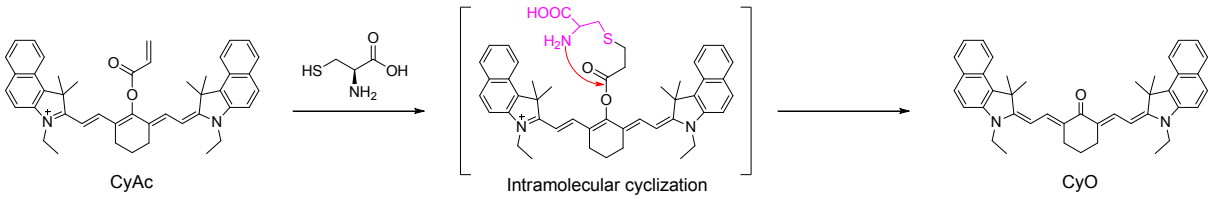

Scheme S2. The proposed mechanism of CyAc for the detection of Cys.

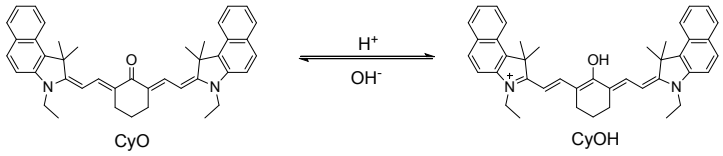

Scheme S3. The proposed mechanism of CyAc with Cys upon the addition H^+.

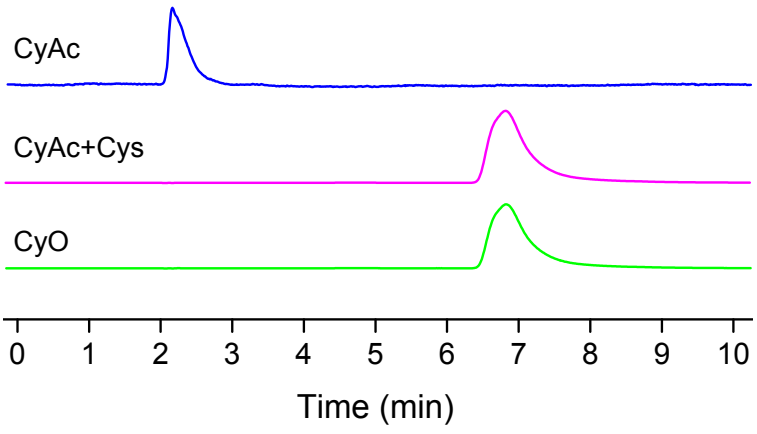

Fig. S10. HPLC chromatograms of CyAc, in the CyAc + Cys, CyO. The mobile phase: solvent A (CH_3CN), solvent B (water), A/B = 7/3.

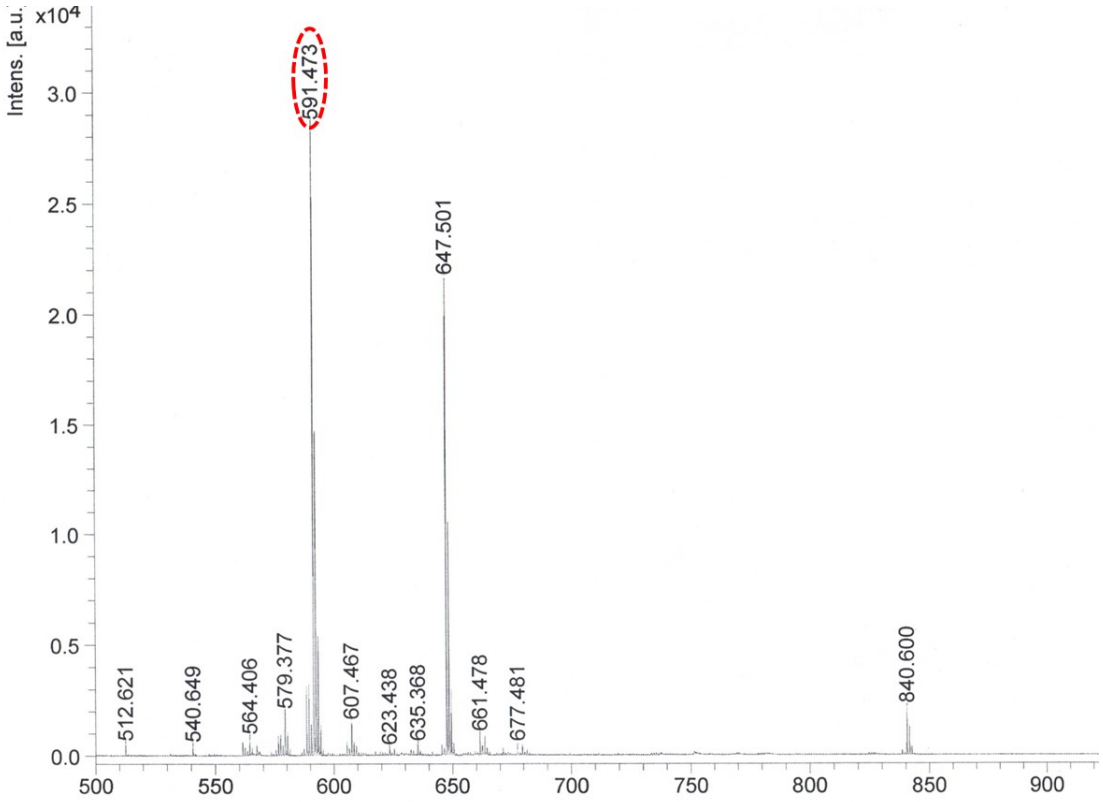

Fig. S11. Mass spectra of CyAc + Cys.

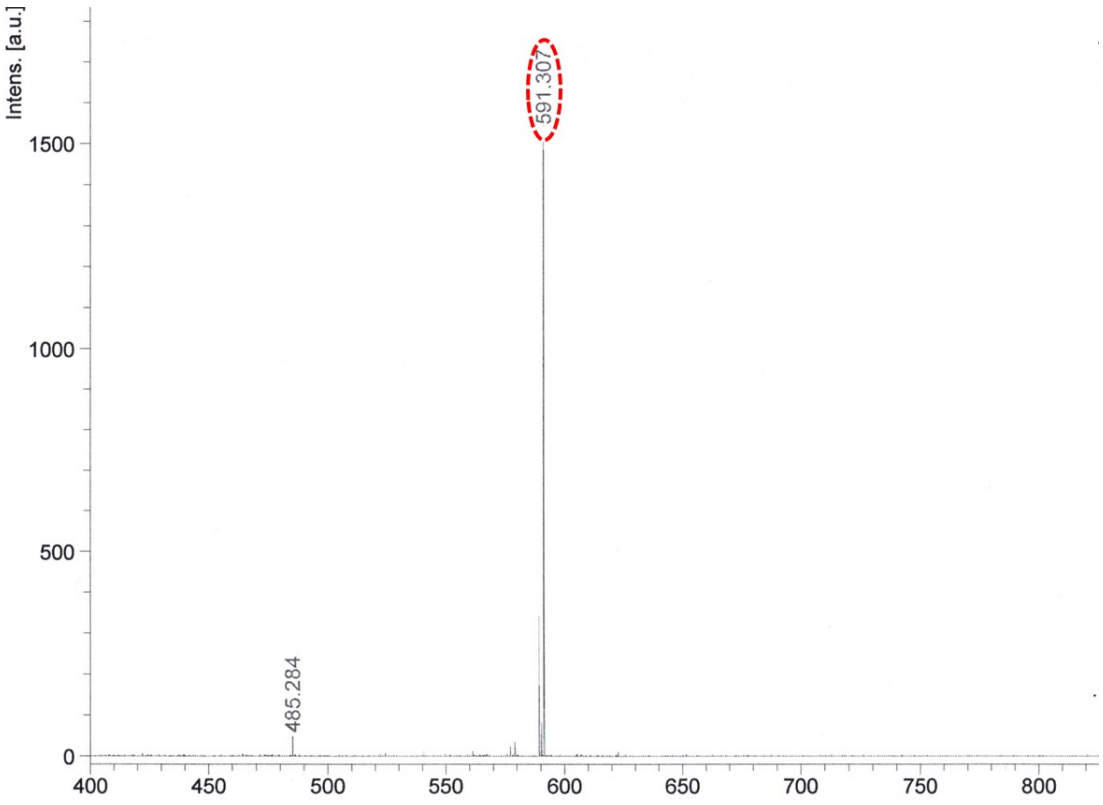

Fig. S12. Mass spectra of CyO.

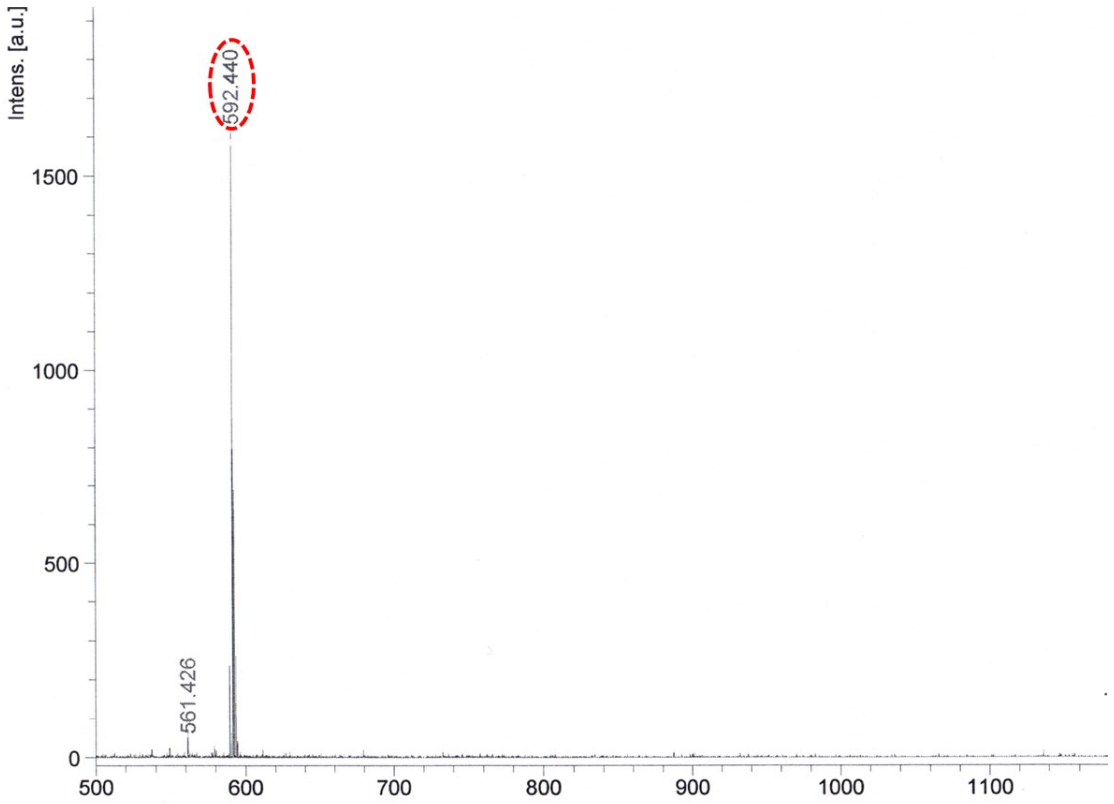

Fig. S13. Mass spectra of CyAc + Cys + H^+.

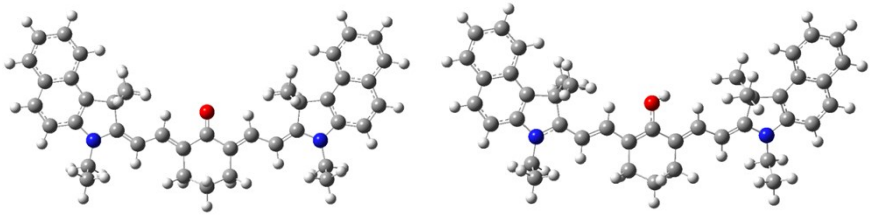

CyO CyOH

Fig. S14. The optimized structures of CyO and CyOH. In the ball-and-stick model, carbon, oxygen and nitrogen atoms are colored in gray, red and blue, respectively.

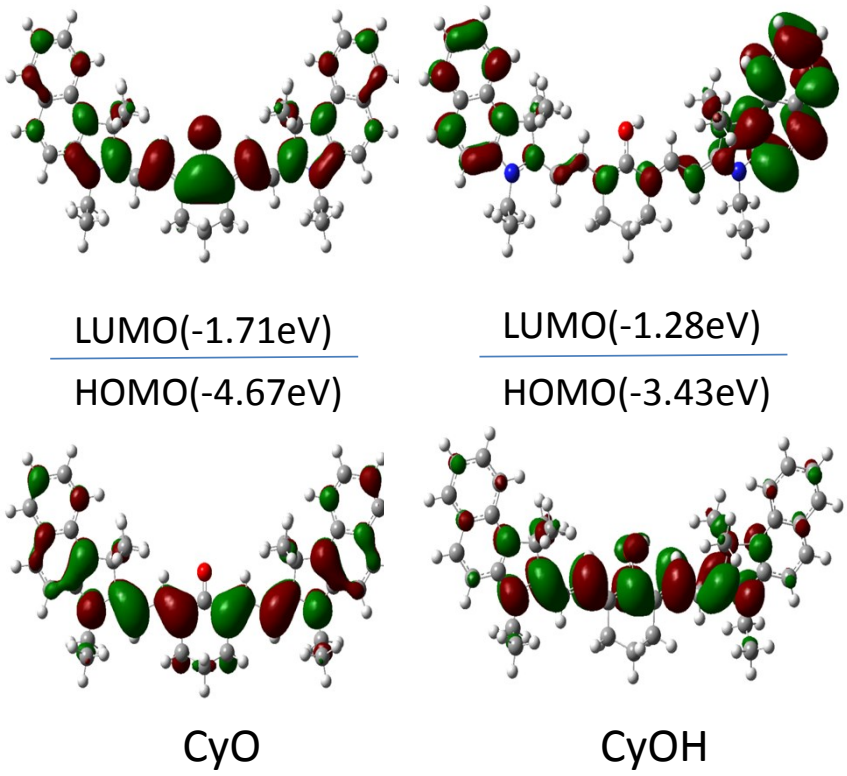

Fig. S15. Frontier molecular orbitals of CyO and CyOH.

5. Biological assays.

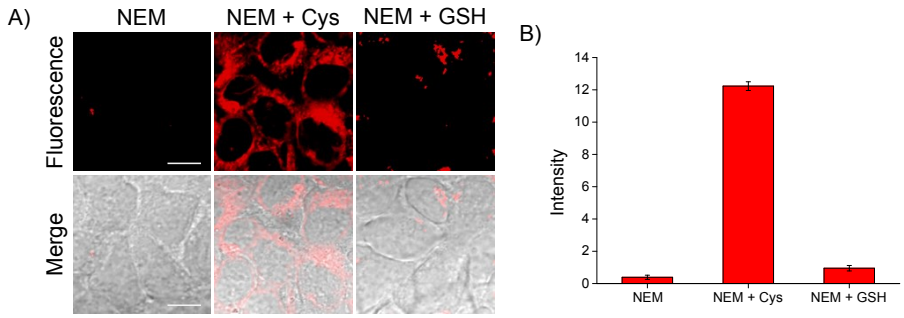

Fig. S16. (A) Fluorescence images of HCT116 cells treated with NEM (200 μM) and CyAc (10 μM). The cells were treated with NEM (200 μM), CyAc (10 μM) and then Cys (50 μM) or GSH (500 μM). (B) Quantification analysis of A. Scale bar: 10 μm. λ_{ex} = 560 nm, λ_{em} = 580-680 nm.

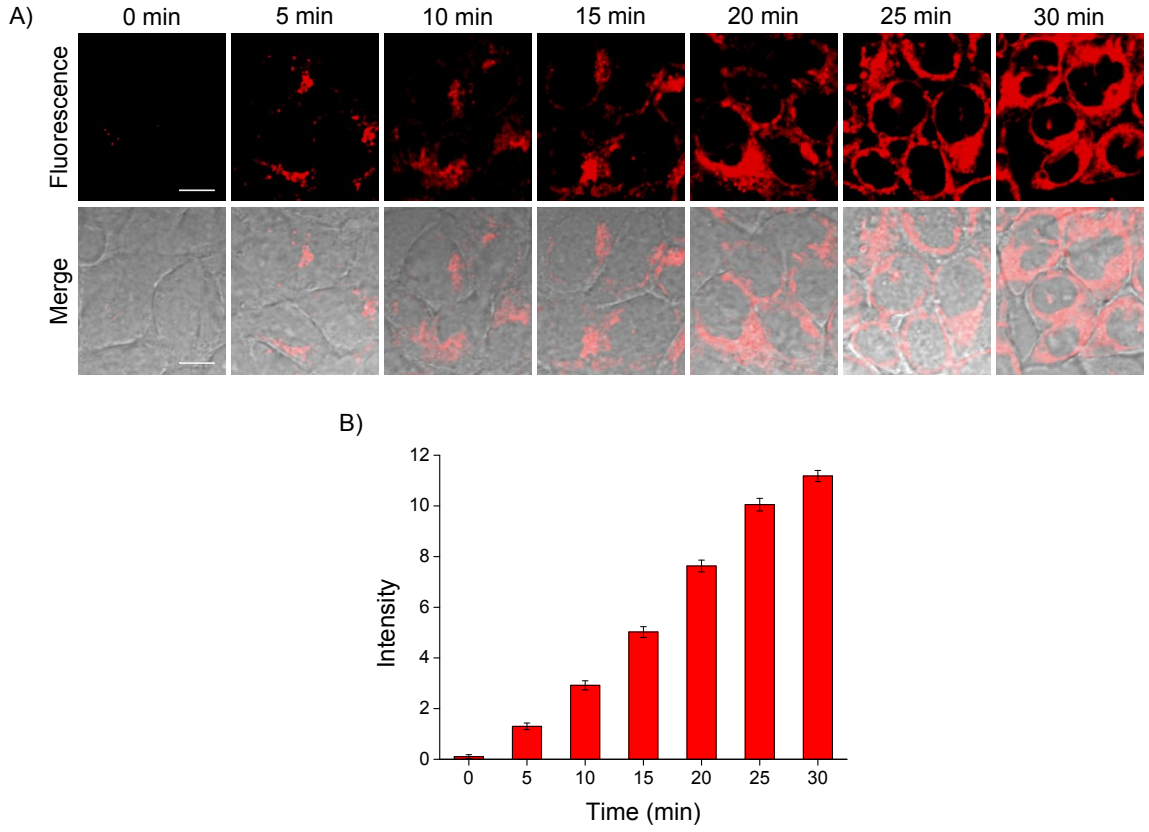

Fig. S17. (A) Fluorescence images of CyAc (10 μM) in HCT116 cells with time (0-30 min). (B) Quantification analysis of A. Scale bar: 10 μm. λ_{ex} = 640 nm, λ_{em} = 750-850 nm.

The cytotoxicity of CyAc in FHC cells and HCT116 cells was test by MTT assay (Fig. S18). After the cells are treated with various concentrations of CyAc from 0 to 50.0 μM, high cell viability is observed, displaying the minimal cytotoxicity of CyAc. Clearly, the probe has good biocompatibility, which provides the possibility for further biological applications.

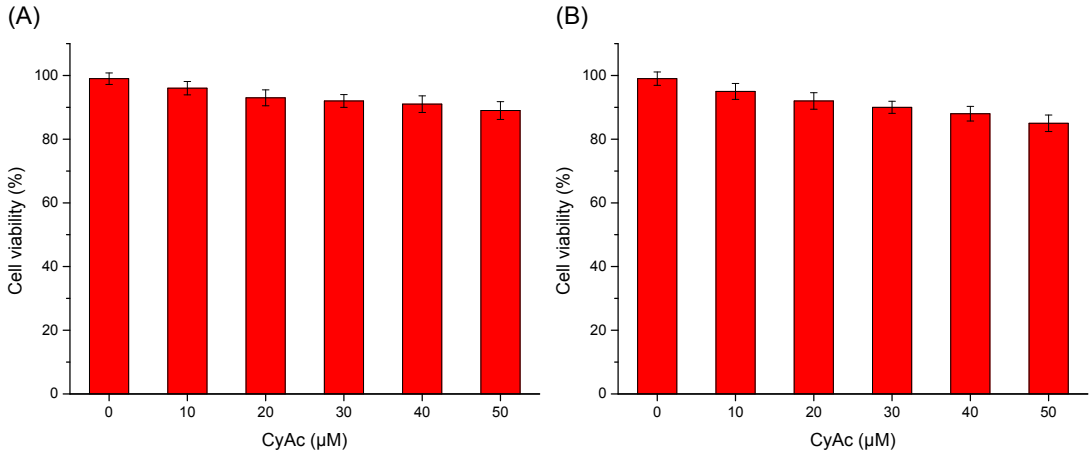

Fig. S18. MTT assay for estimating cell viability (%) of (A) HCT116 cells and (B) FHC cells were treated with various concentrations of CyAc (0-50 μM). Data are shown as mean ± s.d., n = 3.

On the basis of the probes' NIR optical properties and the above cells imaging of Cys and H^+, CyAc was utilized to monitor Cys and H^+ in living mice. As displayed in Fig. S19, the normal mice is given an subcutaneous injection of CyAc, inhibiting very weak fluorescence. While, in the HCT116 tumor-bearing mice given an subcutaneous injection of CyAc, there is intense NIR fluorescence signal in the tumor site. These results show that CyAc can discriminate normal and cancer cells accurately, and thus is suitable for early diagnoses of cancer. In addition, $NaHCO_3$ was injected into the tumor of mice to make the tumor microenvironment be in a neutral condition. As expected, there is almost no fluorescence signal in the tumor. At the same time, the mice were injected with NEM to lower

Cys concentration and no NIR fluorescence signal is shown in the tumor. These results confirm that the NIR probe could be activated by cysteine and H^+ sequentially in the tumor mice, and provide the possibility for cancer diagnosis early and accurately.

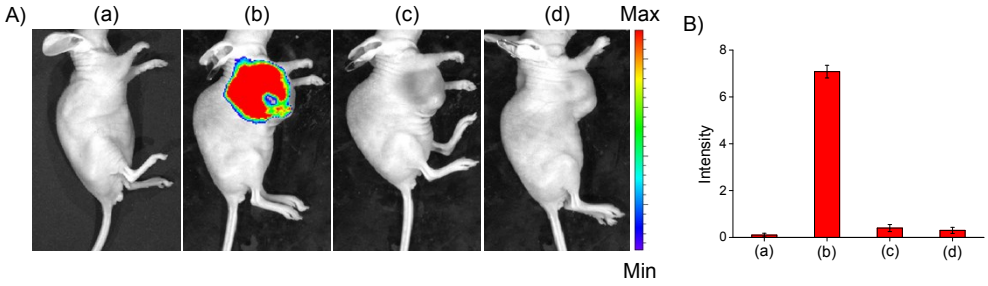

Fig. S19. (A) Fluorescence images of CyAc in mice. (a) The normal mice and (b) the HCT116 tumor-bearing mice were injected with CyAc (10 μM) for 0.5 h. The HCT116 tumor-bearing mice were injected with (c) $NaHCO_3$ (200 μM) or (d) NEM (200 μM) for 1 h and then injected with CyAc for 0.5 h. (B) Quantification analysis of A. λ_{ex} = 640 nm, λ_{em} = 750-850 nm.